

Electrostatic Inkjet Phenomena in Pin-to-Plate Discharge System

Hiroyuki Kawamoto, Kenji Arai and Ryuta Koizumi
Department of Mechanical Engineering, Waseda University
Shinjuku, Tokyo, Japan

Abstract

A preliminary investigation was conducted on electrostatic inkjet phenomena. High voltage was applied between an insulative capillary tube filled with ion-conductive water and a metal plate electrode. Inkjet phenomenon was observed at the dark discharge under conditions of appropriate voltage application and water level. Although the electrostatic attractive Coulomb force is small, in the order of 10 μN at the voltage lower than the corona onset, it is large enough to separate a water drop against surface tension to the capillary tube at certain conditions. The diameter of the drop was about one millimeter. At the beginning of corona discharge, however, water mist was dispersed at wide angle from the tip of the tube due to the Coulomb repulsive force of charged mist. When the applied voltage was further increased, water mist became to be dispersed like spray, because the ionic wind prevented the separation and spread of the droplet. Application of adjusted pulse voltage can form a droplet of which formation is synchronized with the pulse. The diameter of the droplet depended on the applied voltage and the tube diameter. The droplet volume was in the order of several hundred picoliters. Preliminary printing on a paper was also demonstrated. This phenomenon is expected to be utilized for a new inkjet print head.

Introduction

Electrostatics of a pin-to-plate gas discharge system has been widely investigated mainly in the field of the high voltage engineering. However, no systematic study had been conducted for kinetics of the system except for the measurement of corona-induced force per hanging water drop from a high voltage transmission line and ionic wind in the mechanism of corona induced vibration.¹ The authors have been studying kinetics of the system, because it is an important basis for some issues in electrophotography, such as dynamics of a brush or pin charger and a "bead carry-out" phenomenon of a magnetic brush development subsystem.² Another interest is an inkjet system. When a tube filled with ink is used for the pin electrode, an electrostatic inkjet phenomenon is observed. It is expected to be applied for not only the inkjet printing system but also biological analytical chemistry and film formation for microelectronic devices.³

The inkjet printing is currently dominated by thermal and piezoelectric technologies. If the formation of ink droplets can be controlled by the application of the electrostatic field to the liquid, another new print head is expected to be realized. Because preceding researches on the electrostatic inkjet were mainly conducted for the industrial application and the basic research is not enough,^{4,5} we have conducted a fundamental investigation on the formation of the droplet in the electrostatic field. The inkjet printing was also demonstrated utilizing this phenomenon.

Experimental

An experimental set-up illustrated in Fig. 1 was constructed to investigate characteristics of the formation of water droplets. The capillary tube made of silica coated by polyimide (PolymicroTechnologies, Phoenix, AZ) equipped with a bottom of a syringe. Two kinds of the tube were used for experiments; one was 50 μm inner and 170 μm outer diameters and another was 100 μm inner and 170 μm outer diameters. Although the preceding researches were conducted with a metal tube,^{4,5} we used an insulating tube for simplification of the phenomenon as the electrostatic force acted on water only. Ion-conductive water was poured in the syringe and injected into the insulating tube. This tube with water was hanged down perpendicular to a plate electrode made of stainless steel. DC voltage was applied by a DC power supply (Matsusada Precision Inc, Tokyo, HVR-10P) and pulse voltage was generated with a function generator (IWATSU, Tokyo, SG-4105) and a high voltage amplifier (Matsusada Precision Inc, HEOP-10B2). The current was measured by the voltage drop in a current-shunt resistor. The formation of droplet was observed with a digital microscope camera (Keyence, Tokyo, VH-7000). A high-speed microscope camera (REDLAKE MASD, San Diego, CA, Motion-Meter 1140-0003) was also used to observe transient phenomena. The gap was adjusted by a z-stage and the plate electrode was moved in x and y directions with two linear motors to demonstrate the inkjet printing.

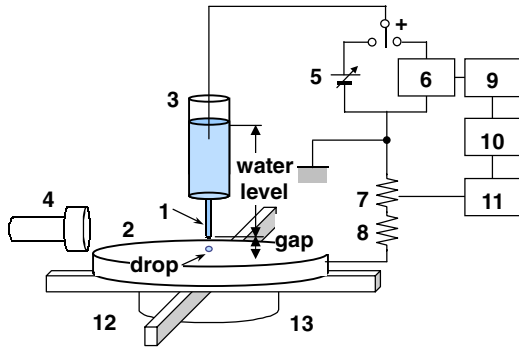


Figure 1. Experimental set-up. (1: water pin electrode, insulative capillary tube filled with water, 2: metal plate electrode, 3: water tank, 4: CCD camera, 5: DC high voltage power supply, 6: high voltage amplifier, 7: shunt resistor, 400 k Ω , 8: resistor: 400 k Ω , 9: function generator, 10: oscilloscope, 11: volt meter, 12: linear stages (x and y directions) 13: mechanical z-stage)

Fundamental Characteristics

In the first place, the current-voltage characteristic of the water pin electrode was measured and it was compared with that of the metal pin electrode of which diameter was the same with the inner diameter of the insulative tube. The results are shown in Fig. 2. Although corona current of the water pin electrode was only half compared to that of the metal pin electrode, probably due to the difference of tip curvature and/or charge of the tube, fundamental characteristics of the discharge were common. That is, no current flowed at dark discharge, however, when the applied voltage reached a threshold (2 kV), the corona discharge took place and the corona current in the order of μA flowed.

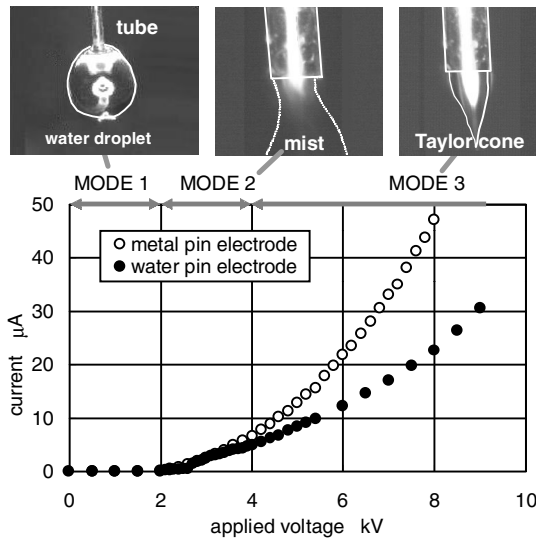


Figure 2. V-I curves in pin-to-plate electrode system. (90 mm water level, $\phi 100 \mu\text{m}$ inner tube diameter, $\phi 100 \mu\text{m}$ metal pin diameter, 3 mm air gap)

As added in Fig. 2 the formation of the droplet was classified into the following three modes corresponding to the discharge modes.

MODE 1 At the dark discharge region, 0 ~ 2 kV, a drop was formed at the tip of the tube. This became large gradually and drops finally.

MODE 2 At the beginning of the corona discharge, 2 ~ 4 kV, water mist consisted of μm order small droplets was dispersed at wide angle from the tip of the tube.⁶ Mode of the mist formation was unstable.

MODE 3 At higher voltage, a Taylor cone⁷ was formed at the tip of the tube, and the cone broke to form a relatively small droplet periodically.

At Dark Discharge Region

Critical Water Level and Voltage of Drop Separation

Figure 3 shows the critical water level, the length between top level of water in the syringe and the lower end of the tube, and the critical applied voltage just when the drop separated from the tube at the dark discharge region (MODE 1). It is evident that the drop was formed under conditions of high pressure and high electrostatic field.

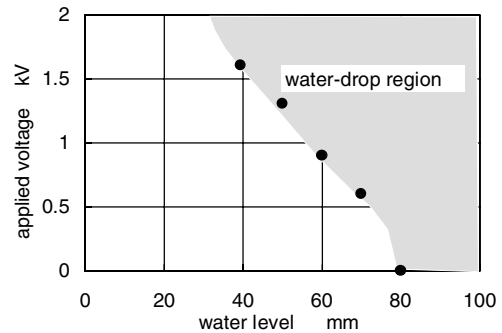


Figure 3. Critical water level and voltage of water dropping at dark discharge. (3 mm air gap, $\phi 100 \mu\text{m}$ inner tube diameter)

Critical Diameter of Drop

Figures 4, 5, and 6 show how the drop diameter at the separation from the tube was determined by the applied voltage, the gap, and the water level, respectively. The critical diameter was small under conditions of high voltage and small gap. This means that the electrostatic force applied to the drop forced to separate the drop from the tip of the tube before it grew up.

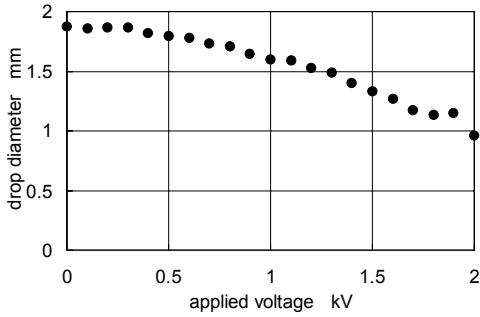


Figure 4. Applied voltage vs. critical diameter of drop at dark discharge. (3 mm air gap, 90 mm water level, ϕ 100 μ m inner tube diameter)

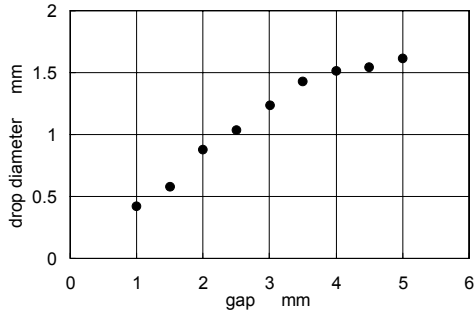


Figure 5. Air gap vs. critical diameter of drop at dark discharge. (90 mm water level, ϕ 100 μ m inner tube diameter, 1.6-kV applied voltage)

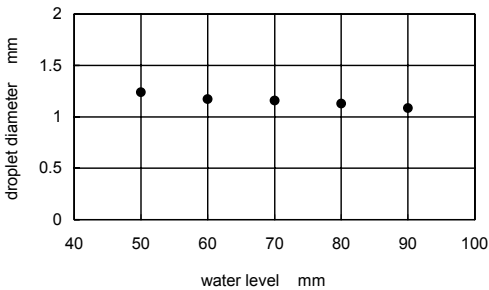


Figure 6. Water level vs. critical diameter of drop at dark discharge. (3 mm air gap, ϕ 100 μ m inner tube diameter, 1.6 kV applied voltage)

Balance of Forces Applied to Drop

In the dark discharge region, forces applied to the drop at the tip of the tube are the electrostatic Coulomb force F_e , force due to surface tension F_s , force due to water pressure F_p , and weight of the drop mg . It is assumed that the critical diameter was determined as a static balance of these forces.

$$F_e = F_s - F_p - mg = 2\pi r_o \gamma - \pi r_i^2 \rho g h - \frac{4}{3} \pi r_d^3 \rho g, \quad (1)$$

where r_o is the outer radius of the tube, 150 μ m, γ is surface tension of water, r_i is the inner radius of the tube, ρ is the density of water, h is the water level, and g designates the gravitational constant. To confirm this hypothesis the electrostatic force F_e was derived from the substitution of criti-

cal condition into Eq. (1) and it was compared with the force separately measured with the metal pin electrode. Experimental method to measure the force applied to the metal electrode was reported in Ref. 8. Here, the diameter of the pin electrode, ϕ 1.2 mm, was adjusted to be approximately same with that of the drop. It is clearly recognized from the result shown in Fig. 7 that the force derived from the critical drop agreed well with that of the metal pin electrode and they were proportional to the square of the applied voltage. From this experimental evidence it is concluded that the critical diameter was determined as a static balance of the Coulomb force, the surface tension, the water pressure, and the gravity.

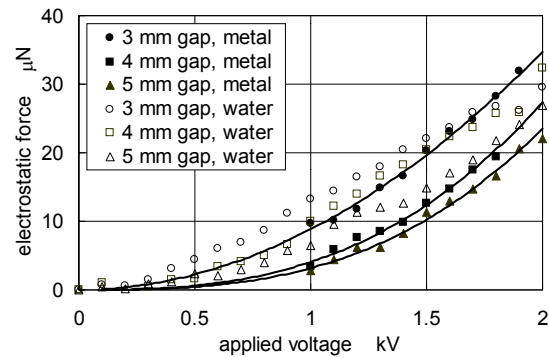


Figure 7. Electrostatic Coulomb force applied to water drop and metal electrode at dark discharge. Solid lines are least-square fitted quadratic curves of the metal electrode. (ϕ 1.2 mm metal pin diameter)

At Corona Discharge Region

At the Beginning of Corona Discharge

Current corresponding to formation of water mist (MODE 2) at the beginning of corona discharge was measured to investigate correlation between the mist formation and the corona discharge. An example was shown in Fig. 8. Pulse current was superposed on the corona current, 0.2 μ A. It is assumed that the Coulomb repulsive force broke the drop in pieces and charged droplets of the common polarity spread along the electrostatic flux line. Because ionic wind is very weak in this region, no substantial bundling force was applied to the mist. However, the mode of the mist formation was very unstable in this region. The mist did not spread in wide angle and/or the mist formation was not periodical but random depending on parameters such as the applied voltage and the gap. Fluctuation of current due to the streamer corona is one of possible reasons.⁹ Further investigation is necessary on the mechanism of mist formation, for it is expected that the MODE 2 is utilized for a micro mist spray and the formation of the extremely small droplet.

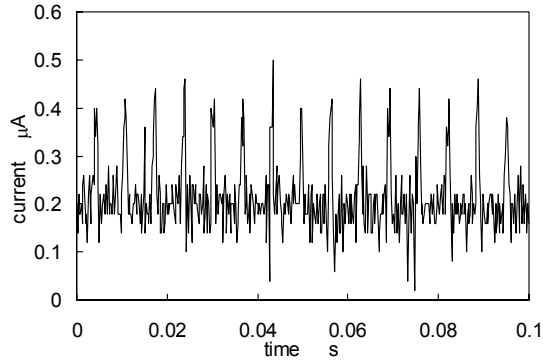


Figure 8. Current corresponding to formation of water mist at the beginning of corona discharge. (3 mm air gap, 90 mm water level, ϕ 100 μ m inner tube diameter, 2.3 kV applied voltage)

At Stable Corona Discharge Region

At higher voltage, more than 4 kV, periodical spike current was observed as shown in Fig. 9 corresponding to the periodical formation of small droplets. It is assumed that convection of the charged droplet is the cause of the spike current. This is confirmed by a synchronized measurement of current and high speed photographing of the droplet formation. The result is shown in Fig. 10. It was observed that the current was slightly increased due to the growth of the droplet and therefore shortening the gap and then suddenly decreased just when the drop separated from the tube. Because substantially strong ionic wind was generated in this region and it streamed to downward from the tip,^{8,9} the charged droplet was not broken nor spread but the single droplet reached to the center of the plate electrode at each cycle.

Relationship between the applied voltage and the frequency of the current pulse was shown in Fig. 11. It seems paradoxical that the droplet formation was less frequent at high voltage application. The reason is probably that repulsive force of the ionic wind to the droplet at the tube tip was high at high voltage but on the other hand attractive force is constant even at high voltage application because the electrostatic field at the tip is maintained constant at the corona discharging.⁸

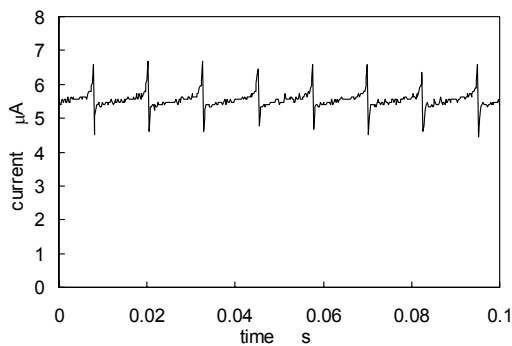


Figure 9. Pulse current corresponding to spraying of water at stable region of corona discharge. (3 mm air gap, 90 mm water level, ϕ 100 μ m inner tube diameter, 4.3 kV applied voltage)

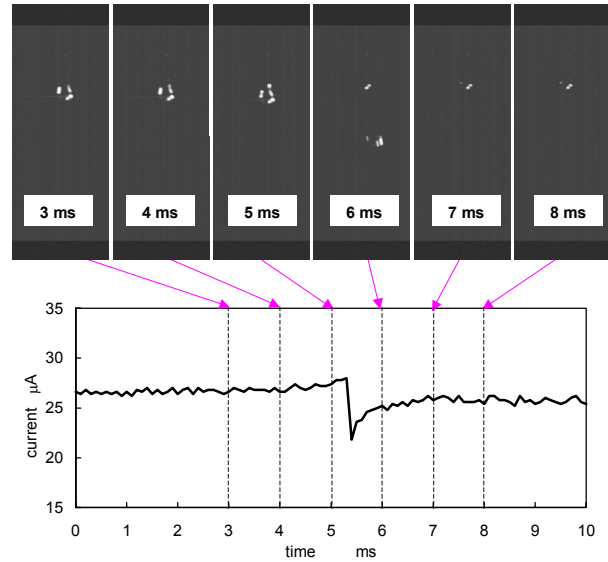


Figure 10. Photograph of dropping of water droplet and corresponding discharge current just at the separation of water droplet. (5 mm air gap, 100- μ m inner tube diameter, 7-kV applied voltage)

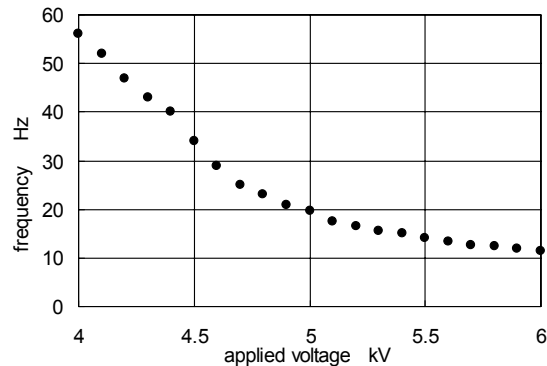


Figure 11. Frequency of current pulse corresponding to spraying of water at stable region of corona discharge. (3 mm air gap, 90 mm water level, ϕ 100 μ m inner tube diameter)

This hypothesis is supported by the experimental result on the droplet size. Measured volume of the droplet was shown in Fig. 12 and 13. (100 pl corresponds to 58 μ m diameter sphere, 1,000 pl to 124 μ m, and 10,000 pl to 267 μ m) Not only the applied voltage but also the gap and the inner diameter of the tube were selected as parameters. First of all, it is evident that the higher the voltage the larger the droplet. Because the repulsive force due to the ionic wind to the droplet prevented the separation of the droplet from the tip of the tube, the droplet grew large before separation under high voltage application. Figure 12 indicated that the droplet volume did not depend on the gap. This evidence also supports the hypothesis, because the repulsive force rarely depends on the gap.⁸

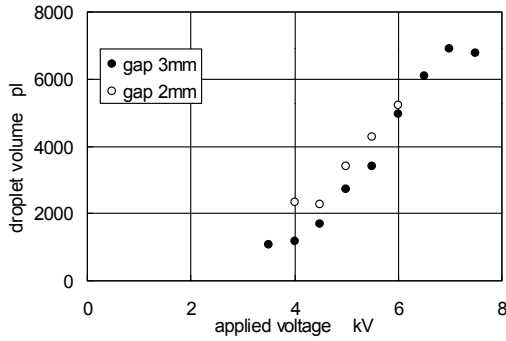


Figure 12. Applied voltage vs. droplet. (90 mm water level, ϕ 100 μ m inner tube diameter, parameter: air gap)

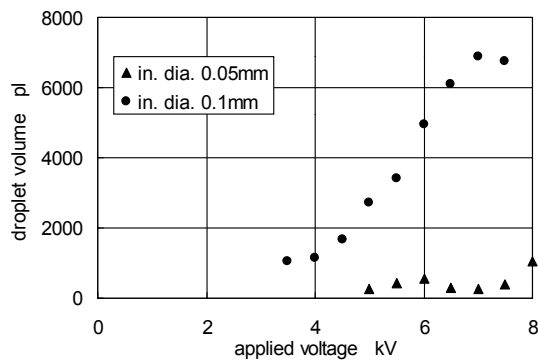


Figure 13. Applied voltage vs. droplet volume. (3 mm air gap, 90 mm water level, parameter: inner tube diameter)

Another experimental result is that the droplet volume was drastically reduced with the tube of the small inner diameter. Parameters must be adjusted to minimize the volume for the practical application of this technology.

Demonstration of Inkjet Printing

For the inkjet printing application, a pulse voltage was applied to control the formation of single droplet. The pulse width with which the single droplet was formed in a pulse was measured at a fixed frequency. The result is shown in Fig. 14. The formation of the single droplet was controlled by the application of the pulse voltage of several tens Hz in the MODE 3 region. The volume of the droplet was in the order of 1,000 pl.

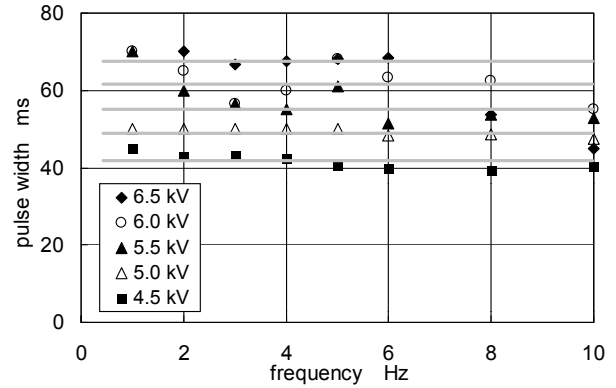


Figure 14. Pulse voltage frequency vs. critical pulse width that separates the droplet from the tip of the tube. (3 mm air gap, 70 mm water level, ϕ 100 μ m inner tube diameter, parameter: applied voltage)

Printing on a paper was demonstrated utilizing this characteristic. A print sample is shown in Fig. 15. Although the present image was preliminary, it is expected to be applied for a new inkjet system.

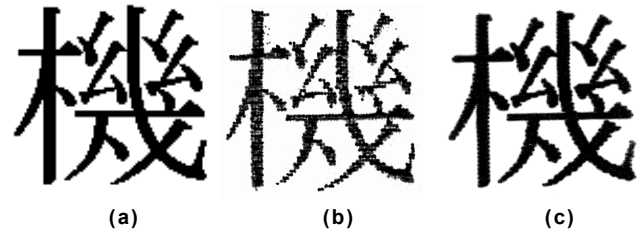


Figure 15. Original (a) and printed samples (b) (c) of Chinese character "Mechanics.". (a) original; (b) 1st stage sample: 50 dpi, 50x50 dots, 100 mm inner tube diameter, 3 mm gap, 4.5 kV applied voltage, dye blue ink for fountain pen; 2nd stage sample: 181 dpi, 100x100 dots, 50 mm inner tube diameter, 0.5 mm gap, 1.5 kV applied voltage, pigmented black ink for Epson inkjet printer

Concluding Remarks

We have investigated electrostatic inkjet phenomena in the gas discharge field between an insulative tube filled with ion-conductive liquid and a plate electrode. The following were deduced from the investigation.

- (1) At the dark discharge region, a relatively large drop is formed at the end of the tube. A critical diameter was determined as a balance of Coulomb force, surface tension, water pressure, and gravity.
- (2) At the first stage of the corona discharge, ink mist was dispersed from the tube.
- (3) At higher voltage, the droplet is sprayed periodically. The frequency of spraying and the size of droplet depend on the applied voltage.

- (4) The spraying of droplet can be controlled with the application of the pulse voltage. Printing of characters on a paper was demonstrated.

Acknowledgements

The authors would like to express their thanks to Kazunori Seki and Hodaka Suzuki for their help of carrying out the investigation. This work is supported by The Asahi Glass Foundation's Research Grant.

References

1. M. Farzaneh and Y. Teisseyre, Mechanical Vibration of H.V. Conductors Induced by Corona: Roles of the Space Charge and Ionic Wind, IEEE Trans. Power Delivery, 3-3 (1988) pp.1122-1130.
2. E. M. Williams, The Physics and Technology of Xerographic Processes, Krieger Publishing Co., Malabar, FL (1993) pp.200.
3. O. Yogi et al, On-Demand Droplet Spotter for Preparing Pico-to Femtoliter Droplets on Surfaces, Anal. Chem, 73 (2001) pp.1896-1902.
4. R. Mills, ESJETTM Printing Technology, IS&T's NIP 12: Int. Conf. on Digital Printing Technologies (1996) pp.262-266.
5. T. Murakami et al, High Definition Ink-jet Printing with Electrostatic Force, J. Imaging Society of Japan, 40-1 (2001) pp.40-47 (in Japanese).

6. J-D. Moon, J-G. Kim and D-H. Lee, Electrophysicochemical Characteristics of a Waterpen Corona Discharge, IEEE Trans. Industry Applications, 34-6 (1998) 1212-1217
7. A. Bailey, Electrostatic Spraying of Liquids, Research Studies Press (1988) pp.60-90.
8. H. Kawamoto, Statics of Pin Corona Charger in Electrophotography, J. Imaging Sci. Technol, 45-6 (2001) pp.556-564.
9. H. Kawamoto, K. Takasaki, H. Yasuda, S. Umezu and K. Arai, Static and Dynamic Phenomena of Pin Electrode in Pin-to-Plate Discharge System, Proc. of the 3rd. IFToMM Int. Micromechanism Sympo. (2001) pp.69-74.

Biography

Hiroyuki Kawamoto holds a BS degree in Electrical Engineering from Hiroshima Univ. (1972) and a Dr. degree in Mechanical Engineering from Tokyo Institute of Technology (1983). From 1972 to 1991 he was a Senior Engineer at the Nuclear Division of Hitachi Ltd. In 1991 he moved to Fuji Xerox, and had been engaged in the research of electrophotography as a Research Fellow. In 1999 he left Fuji Xerox and he is now a professor of Waseda Univ. His awards include the Japan Society of Mechanical Engineers Young Scientist Award (1984), the 7th International Microelectronics Conf. Best Paper Award (1992), the Japan Institute of Invention and Innovation Patent Award (1993), and the 10th International Symposium on Applied Electromagnetics and Mechanics Award for Outstanding Presentation Paper (2001). He was selected a Fellow of the IS&T in 1999.